ARTIFICIAL IMPACT DAMAGE FOR ESTIMATING THE SHORT-TERM RESIDUAL BURST PRESSURE OF COPVS

K. Lasn[1]*, N. P. Vedvik[1], A. T. Echtermeyer[1],
P. Blanc-Vannet[2], O. Bardoux[2],
N. Alexandre[3], F. Nony[3],
F. Dahmene[4], S. Bittendiebel[4],
A. Maldachowska[5], M. Barcikowski[5],
P. Breuer[6], P.-S. Heggem[6]

[1] Norwegian University of Science and Technology, Trondheim, Norway
* e-mail: kaspar.lasn@ntnu.no
[2] Air Liquide Research and Development, Jouy en Josas, France
[3] CEA, DAM, Le Ripault, Monts, France
[4] Institut de Soudure, Yutz, France
[5] Wroclaw University of Technology, Wroclaw, Poland
[6] Hexagon Composites, Raufoss, Norway

Keywords: COPV, Pressure Vessel, Impact, Burst, Residual Strength

ABSTRACT

Composite pressure vessels are vulnerable to mechanical damage from impacts. For vessels operated in the field, the actual impact loads are not known. However, a damaged laminate can be studied by non-destructive testing methods to obtain approximate sizes and locations for the damage. The damage inside the composite can be considered as an assembly of identifiable basic shapes. The configurations of artificial impact damages in the current paper resemble the observed damages from the experiments. In the results, the burst pressure of healthy vessels is slightly overestimated by the current finite element model. The cylinders modeled with artificial impact damages display stress concentrations around the damage, and reduced burst strengths. The delamination size was found to be insignificant for residual burst pressures, meaning that fiber damages are of primary importance.

1 INTRODUCTION

Large composite overwrapped pressure vessels (COPVs) are used to transport gas for industrial purposes. Smaller COPVs are often employed as fuel tanks, containing compressed natural gas or hydrogen for buses, trucks, and cars. Transportable pressure vessels spend their life in a more unpredictable environment compared to stationary vessels, and are therefore more susceptible to mechanical damage e.g. from impacts.

The damage from mechanical impacts is a serious concern for the safety of composite pressure vessels. An important question is how much impact damage can be tolerated before the short-term burst strength degrades. Physical impact testing is carried out to assure and validate the safety of COPVs. In the HyPactor project [1], both empty and pressurized vessels were subjected to physical impact experiments. For the latter case, the pressure inside the cylinders was 700 bar i.e. the nominal working pressure at 15°C for these cylinders. All of the tested vessels were investigated visually, and a selection of vessels with acoustic emission, ultrasound c-scans and x-ray tomography. The information from non-destructive testing (NDT) helps to evaluate the underlying mechanisms which cause reductions in the residual burst performance.

Current work employs a finite element (FE) model to calculate the residual performance. The residual burst pressures are evaluated for a number of artificial damage configurations. These configurations represent approximations of damages, which have been observed in impact tested vessels from physical experiments. The observed damage of empty vessels was slightly different than

the damage on pressurized vessels. The FE model produced a satisfactory agreement between predicted and measured burst pressure for the healthy vessel and showed a reduction of performance for vessels with impact damage. The effect of delaminations and fiber damage on the external and the internal surface, is discussed.

2 PREVIOUS STUDIES ON IMPACT ON PRESSURE VESSELS

Composite pressure vessel design and the impact damage in composites has been the focus of many investigations. The level of detail in the predictions and calculations continues to be improved with advances in numerical modelling. In a selection of recent modelling work [2-5], all researches employed a ply based 3D FE model with Hashin failure criteria to study impacts and the residual strength of pressure vessels. Cohesive zone modelling is often employed to evaluate delaminations between individual plies. There are differences in the failure criteria used for other failure mechanisms besides the fiber tensile failure. Interestingly, the damage model in [2] also considers the statistical variation of composite strength. The main issues with the modelling are the lack of input information and the model validation. The models are complex, especially regarding the dome region, and considering how various failure mechanisms are being implemented. Full confidence in the output from modelling has not been established yet. The information about the build-up of commercial vessels is typically confidential. In addition, the properties of filament wound composite are different from flat laminates and therefore not easily available.

In parallel to the modelling, some exterimental work has been conducted. The experiments have showed that autofrettage improves the impact resistance of *Type III* carbon fiber/epoxy cylinders [6]. Damages were inhibited due to residual tensile stresses in the composite. The cylinders absorbed less energy from the impactor, the residual burst strength was increased, and the residual fatigue life extended. The damage progression in a cylindrical composite-metallic structure was experimentally investigated in [7]. A quasi-static indentation test was interrupted at selected points along the load path, specimen was unloaded and *ex situ* micro-focus computed tomography was employed for the damage assessment. The sequence of damage progression in the CFRP shell was: matrix cracking, followed by delamination forming a pine-tree damage profile with an undamaged central cone. The first fiber fracture occurred in the outermost layers, directly under the loading nose, accompanied by severe delaminations around it. A recent summary of experimental work [8] analyzes over 200 impact test results from various cylinders and manufacturers and concludes that the (normalized) absorbed energy, i.e. the energy lost by the impactor during the impact, is a good metric to define the threshold where the short-term residual burst performance begins to become reduced. The energy absorbed by unpressurized vessels was ca. 80% of the incident energy, whereas only ca. 60% for the vessels impacted under service pressure. The difference was attributed to the global inelastic deformation of the structure, since empty vessels behave less rigid than pressurized vessels, under impact.

Numerical and experimental research is often conducted with thin composite tubes and/or impact energies that rarely exceed a few hundred joules. The experimental work shows that increasing the incident energy of the impactor reduces the residual burst strength of the vessel, with a possible threshold in the lower impact energy region. This threshold may be related to the initiation of fiber failures, but a detailed explanation does not yet exist. When pressure vessels are impacted under internal pressure, global deformations are reduced and the damage occurs more locally, near the impacted region. Somewhat similar effect is noticed from autofrettage – increased bending stiffness inhibits the damage from the impact. Fiber failures are considered of primary importance, directly linking to the residual performance, whereas the effect of delaminations on the residual performance is a bit unclear. Matrix cracking is typically disregarded. It is important to point out that fiber failures inside the vessel shell (other than vessel surface) are difficult to assess by common NDT methods.

- Delaminations shield the damaged area for ultrasonic C-scans.
- X-ray tomography at current state requires cutting of the specimens to achieve required resolution.

- Acoustic emission gives the global location of damage, but does not give detailed through-thickness locations for specific damage types. Further, it records only new damage, but says little about existing damages.

Current work aims to improve the understanding of short-term residual burst performance. Artificial damage configurations are implemented into the numerical model to simulate impact damage from empty and pressurized vessels. Further, the effects from individual basic damage components are evaluated.

3 THE FE MODEL

The 3D FE model is created in Abaqus/Explicit, suitable for modelling high-speed impact events where material degradation, failure, and inertia play a significant role. Mass scaling can be utilized for quasi-static loading, i.e. for the pressurization of the cylinder. Overall, the current FE model is an improved version of earlier work [5].

3.1 Geometry

The pressure vessel is modelled as a cylindrical structure, as seen in Figure 1. The domes are simplified as isotropic disks, closing the ends, flush with the external surface of the composite. It is possible to simulate impacts, but this is not the focus of current paper. The hemispherical impactor is modelled as rigid and strikes the vessel at the chosen location. Further details of the model are shown in Figure 2. The tube is composed of an isotropic liner with plasticity included, and concentric layers of composite plies. In the coarsely meshed areas away from the impact region, the composite is homogenized and purely elastic. At the impact location, the composite has a layer-by-layer discretization, allowing for fibre failure, matrix damage, and delamination damage. The edge region of the fine-mesh composite is elastic (without damage evolution) to the extent of 1.3 composite thicknesses, as shown in Figure 2. This modelling approach facilitates the stress transition between different mesh densities, reducing artificial damage at the edges.

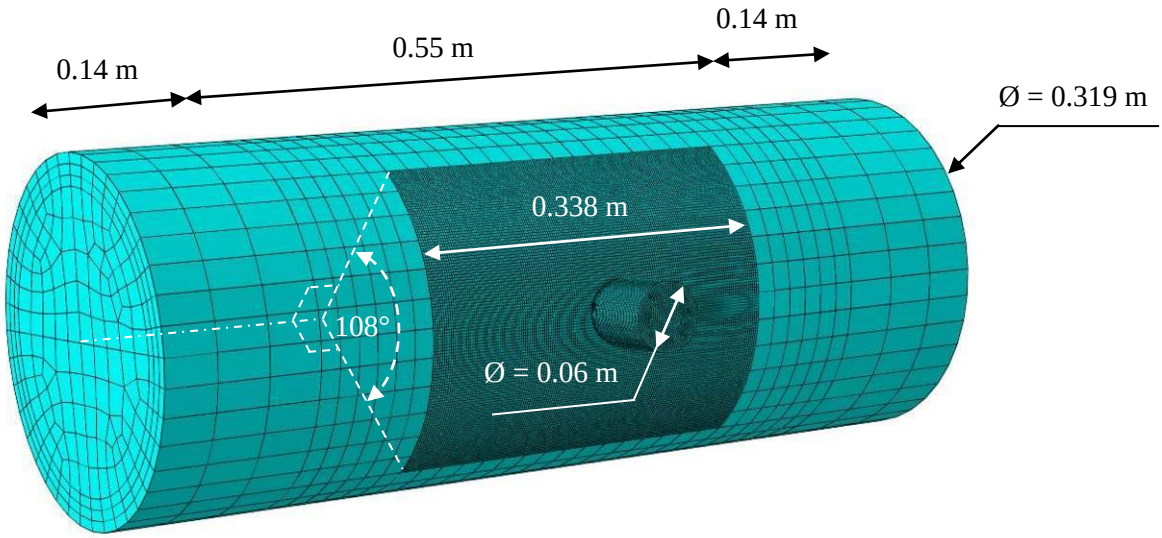

Figure 1: The geometry of the FE model.

3.2 Boundary conditions and loading

During pressurizations, the cylinder is fixed at the external flat surface of one dome. The pressure loading is applied onto the internal surface of the liner and on the corresponding internal surfaces of dome-disks. The pressure is increased from one level to the next in a smooth step amplitude definition, with an average pressurising speed of 2000 MPa/s. Thereby, pressurising from 0 to 2000 bar takes place in 0.1 s. Tie constraints are employed to assemble the various constructs of the model into a

single structure. Contact interactions are defined for individual plies which may establish contact during the progressive failure of the composite shell. Hard contact is assigned for the normal behaviour and a friction coefficient 0.3 for tangential movements. The default bulk viscosity with linear and quadratic parameters 0.06 and 1.2 respectively, was used. Mass scaling makes the quasi-static analyses more economical, but only for steps not involving the impact event, where the inertia needs to be accurately accounted for. Mass scaling was applied by the stable time increment STI = $3 \cdot 10^{-7}$ s for elements whose STI was below this value.

3.3 Mesh

The FE model is composed of rigid quadrilaterals, linear brick elements and quadrilateral continuum shells, as detailed with Abaqus element notations in Figure 2. The composite plies in the impact region are composed of a single element per layer, and separated by zero thickness cohesive elements. The constitutive thickness of the cohesive elements is chosen as 0.1 mm. The in-plane element size of the coarsely meshed region is approx. 23 mm. The impact region has element sizes 2.1 mm in the axial and 2.1-2.5 mm in the hoop direction, at the inner and outermost ply, respectively. The liner has two elements in the thickness direction.

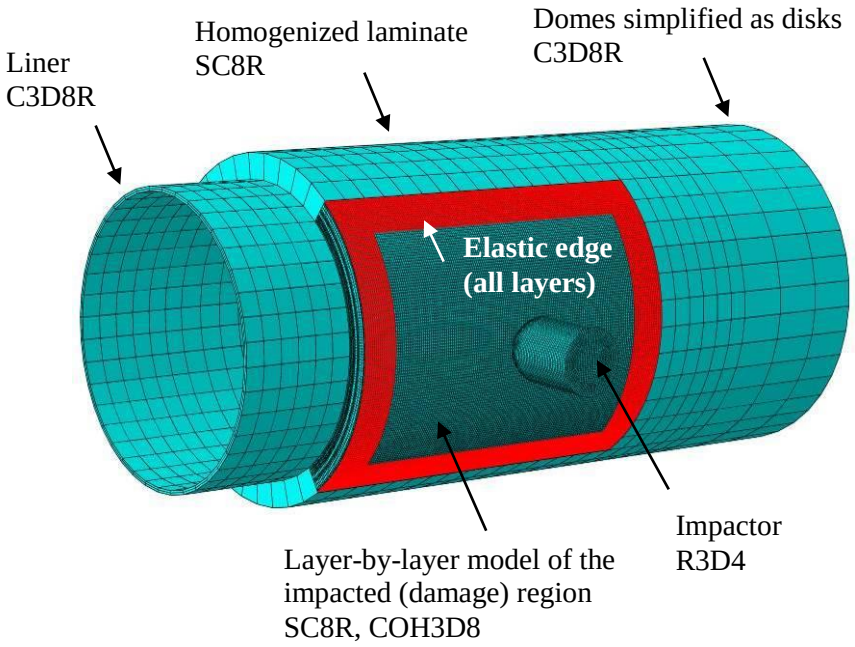

Figure 2: Cross-section of the model.

3.4 Layup

The layup of the composite shell is composed of 18 layers, consisting of hoop (i.e. 90° in relation to the cylinder axis) and two separate helical angle pairs. Hoop and helical layers are modelled with different material input.

3.5 Material properties

The summary of material properties is given in Table 1. The domes are isotropic and linear elastic. The liner material is defined as isotropic, with plastic material behaviour included. The stress based Hashin's failure criterion is defined for the initiation of fibre and matrix damage inside the plies. The coefficient $\alpha = 0$ defines that the shear stress does not contribute to the fiber tensile strength. The evolution of damage is controlled by fracture energies and stabilized by viscous behaviour. Cohesive interfaces are implemented between the individual layers of the composite. The damage in the cohesive elements is initiated by a quadratic stress criterion and the energy based Benzeggagh-Kenane (BK) formulation is used as the fracture criterion.

The composite layers were modelled with continuum shell elements and numerical issues were encountered when these elements were loaded in in-plane biaxial tension with severe through-thickness compression. The shell elements displayed premature failures without reaching their in-plane fiber direction strengths. This issue was overcome by overriding the section properties of through-thickness modulus, through-thickness shear moduli and the Poisson's ratio. The elastic moduli were given very high values, 1000 GPa both, and the section Poisson's ratio a value of 0.0. This necessary step however reduces the realism of through-thickness behaviour in the current model.

Material	Specifics	Notation	Values
Dome	Isotropic properties	ρ_D, E, ν	580 [kg/m^3], 50 [GPa], 0.3 [-]
Liner	Isotropic properties	ρ_L, E, ν	960 [kg/m^3], 1.1 [GPa], 0.45 [-]
	Elastic-plastic behaviour	True yield stress Plastic strain	23.5; 161 [MPa] 0; 1.93 [-]
Composite hoop	Density	ρ_{hoop}	1544 [kg/m^3]
	Elastic constants	E_1, $E_2 = E_3$	137 [GPa], 15.0 [GPa]
		$G_{12} = G_{13}$, G_{23}	4.8 [GPa], 4.2 [GPa]
		$\nu_{12} = \nu_{13}$, ν_{23}	0.30 [-], 0.50 [-]
	Strengths	X_1^T, X_1^C	2620 [MPa], 1470 [MPa]
		X_2^T, X_2^C	55 [MPa], 215 [MPa]
		$X_{12} = X_{13}$, X_{23}	70 [MPa], 60 [MPa]
	Fracture toughness	$G_{tl} = G_{cl}$	62 [kN/m], 62 [kN/m]
		$G_{tt} = G_{ct}$	0.585 [kN/m], 0.585 [kN/m]
	Viscosity coefficient, relaxation time, for all modes	$\eta_{ft}=\eta_{fc}=\eta_{mt}=\eta_{mc}$	10^{-9} [s]
Composite helical	Density	ρ_{hel}	1416 [kg/m^3]
	Elastic constants	E_1, $E_2 = E_3$	93.0 [GPa], 9.0 [GPa]
		$G_{12} = G_{13}$, G_{23}	2.9 [GPa], 2.6 [GPa]
		$\nu_{12} = \nu_{13}$, ν_{23}	0.30 [-], 0.50 [-]
	Strengths	X_1^T, X_1^C	1760 [MPa], 980 [MPa]
		X_2^T, X_2^C	55 [MPa], 215 [MPa]
		$X_{12} = X_{13}$, X_{23}	70 [MPa], 60 [MPa]
	Fracture toughness	$G_{tl} = G_{cl}$	53 [kN/m], 53 [kN/m]
		$G_{tt} = G_{ct}$	0.585 [kN/m], 0.585 [kN/m]
	Viscosity coefficient, relaxation time, for all modes	$\eta_{ft}=\eta_{fc}=\eta_{mt}=\eta_{mc}$	10^{-9} [s]
Cohesive layers	Density	ρ_{COH}	1200 [kg/m^3]
	Stiffness	E_3, $G_{13} = G_{23}$	3.5 [GPa], 1.3 [GPa]
	BK power parameter	η	1.4
	Strengths	τ_n, $\tau_s=\tau_t$	50 [MPa], 50 [MPa]
	Fracture toughness	G_{Ic}, $G_{IIc} = G_{IIIc}$	0.8 [kN/m], 1.8 [kN/m]
	Viscosity coefficient, relaxation time, for all modes	η_{COH}	10^{-9} [s]

Table 1: The material properties.

4 MODELLING AND EXPERIMENTAL RESULTS

4.1 Damage mechanisms

Figure 3 shows a cross section of an empty pressure vessel, deformed under a low velocity impact. The composite endures high multiaxial compressive stresses in the outermost layers, directly under the impactor. Shear and tensile stresses cause delaminations between composite layers, typically when their winding angle changes. Finally, in case of severe bending deformations, the inner surface of the composite becomes subjected to high tensile stresses.

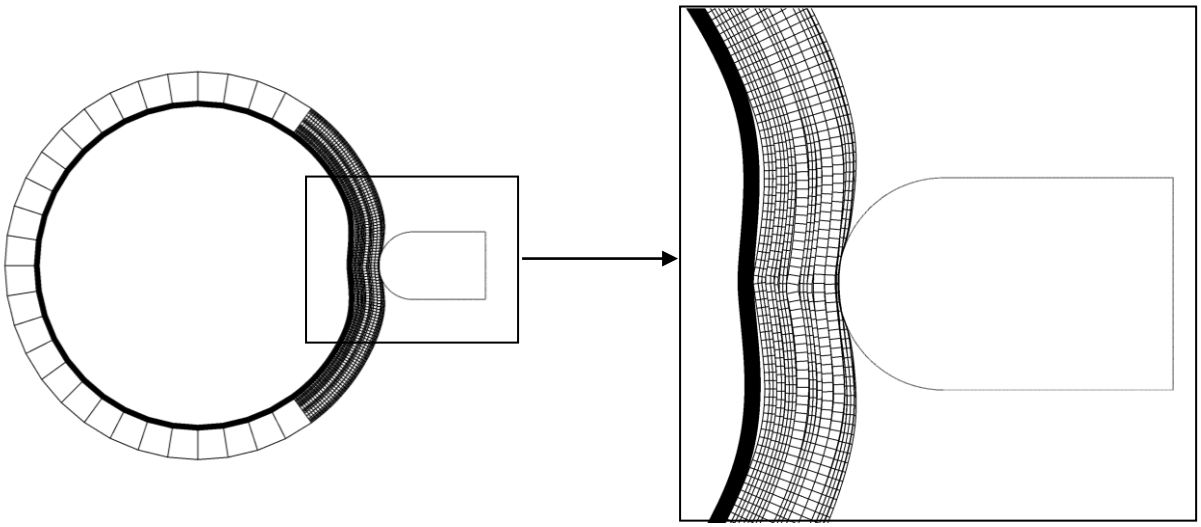

Figure 3: Pressure vessel deformation under impact.

4.2 Experimental observations from HyPactor

A database of impacts has been created in the European project HyPactor [1], in order to provide pass-fail criteria for damaged cylinders. A selection of these pressure vessels was characterized by NDT methods: ultrasonic C-scans, acoustic emission measurements and x-ray tomography. The experimental results (from a single impact onto the middle of the cylinder) indicate the following.

- Increasing the impact energy over a certain threshold reduces the burst pressures and expands the visual markings on the external surface of the composite (damaged area), see Figure 4.
- The delaminations inside the laminate are more extensive for cylinders impacted empty, compared to cylinders impacted under 700 bar pressure, as seen in Figure 5.
- Residual burst pressures indicate that impact on empty cylinders gives comparable/conservative results to cylinders impacted when pressurized at 700 bars.
- Information about fiber failures occurring on the inner surface and their effect on the residual performance is inconclusive.
- High-speed camera footage confirms the hoop failure mode. The fracture of the composite in impacted vessels originates from the impact area and initially develops longitudinally, parallel to the cylinder axis. This means the failure is controlled by the failure of hoop layers.

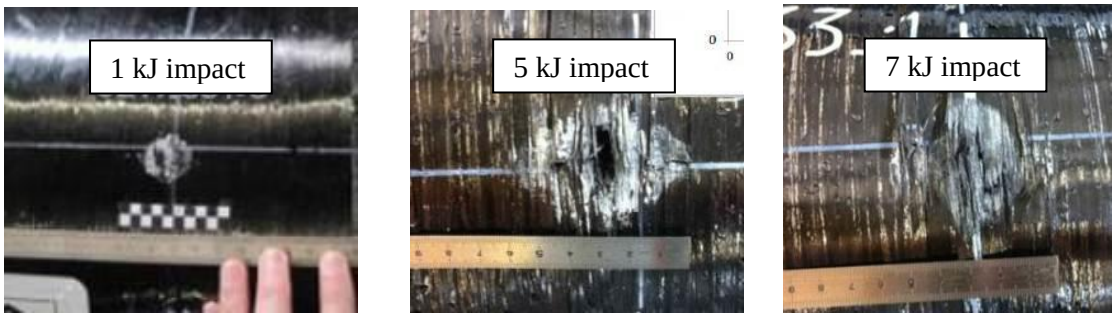

Figure 4: Markings on the external surface from visual inspection.

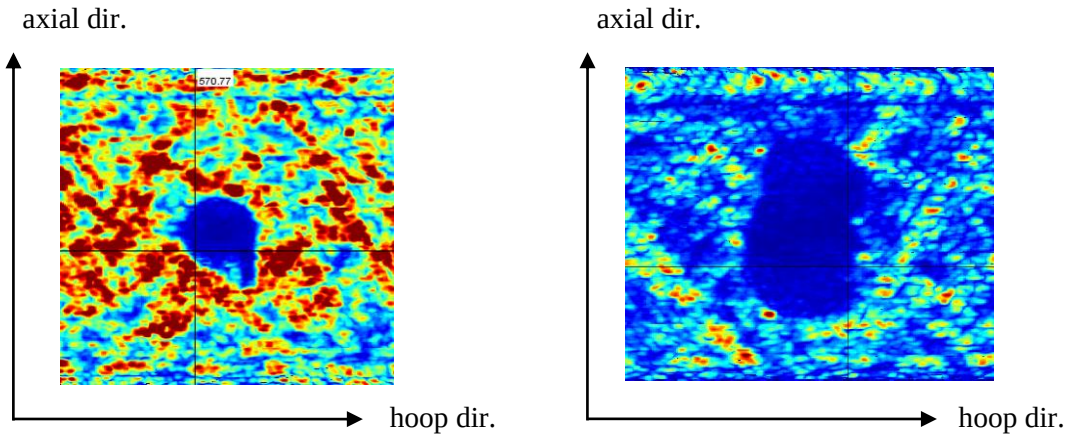

Figure 5: Ultrasound shows the delaminated regions in the cylindrical section of the pressure vessel. The side facing the impactor is shown – full cylindrical length in the axial direction and ca. half of the circumference in the hoop direction.

4.3 Basic damages

In the current work, the focus is not on how the damage is created. Instead, the effects of a given damage on the residual performance of the pressure vessel are studied. This is important, since, for vessels operated in the field, the actual impact loads are not known. However, the damaged laminate can be studied by NDT methods to obtain approximate sizes and locations of the damage.

The composite damage is considered as an assembly of identifiable damages, characterized in terms of basic shapes (ellipses and rectangles) in separate layers of the laminate. The damage is implemented by reducing the stiffness of the selected finite elements to 0.1 % of their initial values (Table 1). All three stiffnesses are reduced in cohesive interface elements. In ply elements, three E moduli and three G moduli are reduced, while Poisson's ratios are kept with initial values. The configurations of ply damages are similar to what has been noted from experiments. The basic damage configurations in this work are summarized in Table 2 and visualized in Figure 6.

Acronym	Description	Damage Size	
		In-plane	Thickness direction
DLS	Small delamination	Ellipse with radii a = 50 mm, b = 50 mm	All interfaces
DLL	Large delamination	Ellipse with radii a = 120 mm, b = 60 mm	All interfaces
FFI	Fiber failure in the internal hoop layer	Rectangular crack a=4.2 mm x b=16.9 mm (2x8 elements)	The innermost hoop layer
FFE	Fiber failures in the external layers	Ellipse with radii a = 15 mm, b = 15 mm	Four external layers (2 hoop, 2 helical)

Table 2: Basic damage configurations.

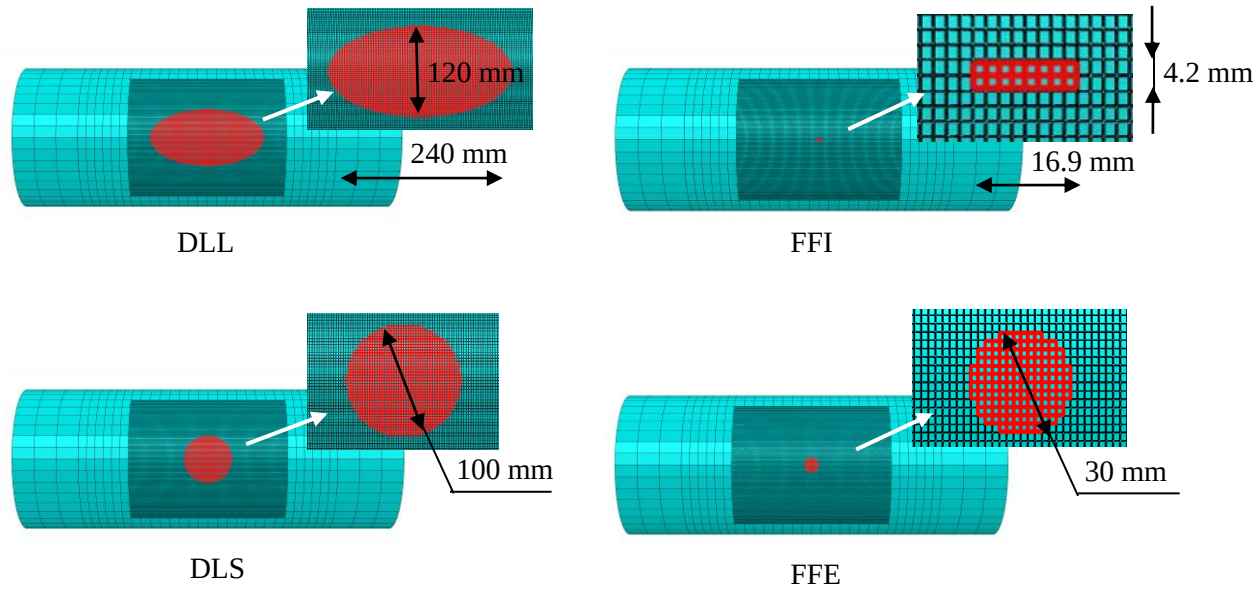

Figure 6: Basic damage configurations.

4.4 Stress redistribution

As artificial damages are introduced into the plies, the stress fields around these damages change. The contours of tensile stresses for two basic damages are shown in Figure 7. The arrows point to the stress concentrations. Artificial delaminations, when considered separately from fiber failures, did not seem to significantly alter the stress fields. The FFE damage essentially removes 24% of all hoop fibers from the circular area of the laminate, and the stresses become redistributed in the thickness direction. That is, other hoop and helical layers under this region become more highly loaded; however they have a bit milder stress concentration, compared to the original damaged ply. This thickness-wise redistribution occurs also for the FFI damage, but to a lesser degree, since the innermost ply accounts for only 14 % of the total thickness of all hoop layers. The final failure is initiated at the location of highest stress concentration, as seen in Figure 7.

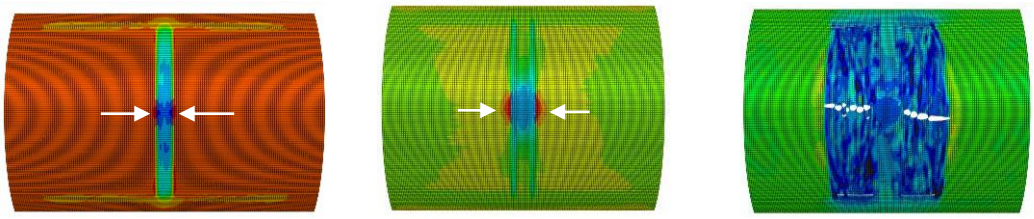

FFI damage
Ply nr. 1

FFE damage
Ply nr. 18

FFE damage
Ply nr. 18
Failure initiated

Figure 7: Stress contours for hoop plies, tensile stresses in the fiber direction. The arrows point to the stress concentrations.

4.5 Burst pressures from 3D FE modelling

The basic damages from the Section 4.3 are now being combined simultaneously, resulting in four damage configurations, besides the healthy reference configuration. The overview of cylinder damage configurations is shown in Table 3. It needs to be pointed out that damages described in Table 3 are artificial, no impact simulations were performed to obtain these configurations. They resemble the observed damages and are therefore approximately based on the input from NDT. Configurations 1, 2 may be thought of as "empty" since empty vessels displayed larger delaminated regions (DLL), as seen from ultrasound images such as Figure 5. Configurations 3, 4 may be considered as "pressurized" due to the smaller delaminated area. The second aspect in consideration is the effect from possible fiber damages in the internal layer (FFI), of which there is little information available.

Configuration nr., applied damages	Burst pressure range, bar	
	Min.	Max.
0) Reference, healthy vessel	1842	1878
1) DLL+FFE+FFI	1365	1439
2) DLL+FFE	1450	1488
3) DLS+FFE	1094	1479
4) DLS+FFE+FFI	1365	1421

Table 3: Burst pressures of cylinders with simulated damage.

The termination of the Explicit simulation in Abaqus software is set by some internal criterion, not necessarily related to the burst event. Before the end of the simulation, there is also the last output frame, where no fiber failures can be seen on the structure. The burst i.e. the progression of fiber failures occurs between these moments in time. The burst pressures in Table 3 are evaluated by this range from the last intact moment (no fiber failures) until the end of the simulation. The precision of this approach depends on the frequency of output variables. The visualization of burst pressures is also shown in Figure 8. Most of the vessels failed suddenly, as all fiber damage occurred within one output frame, at the very end of the analysis. The damage configuration 3 failed in a special manner: half of the external hoop ply failed quite early, however the final burst occurred at a pressure comparable to other damaged vessels.

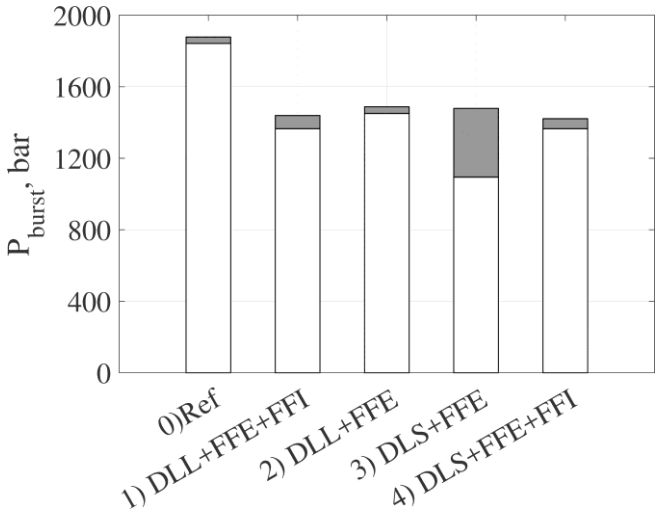

Figure 8: Burst pressures of cylinders with simulated damage.

5 DISCUSSION

The results in Table 3 and Figure 8 show that pressure vessels with artificial damage display reduced burst strengths, as expected. All of the damaged configurations include fiber failures in four of the external plies (FFE). This altered the fibers most and is therefore the dominant effect reducing the residual strength. The size of the delamination (DLL vs DLS) and the additional small crack in the interal hoop layer (FFI) seems to have a secondary effect. Evidently, the size of the delaminations does not significantly change the residual burst pressures.

The stresses inside a thin pressure vessel wall can be considered as uniform in through-thickness direction. This is not the case for thick pressure vessels. For the current cylinder model, hoop tensile stresses are highest in the innermost layer, exceeding the hoop tensile stresses in the outermost layer by ca. 15 %. Therefore, any damage to the innermost layer should have consequences for the structural integrity. From the simulation results, it is evident that the fiber failure added into the internal layer (FFI) did further reduce the burst pressures, compared to configurations without this damage. However, since the external ply damage was the main contributor to damage in this study, the additional small internal damage only has a minor effect on the burst pressure reduction.

6 CONCLUSIONS

A 3D FE model has been developed for calculating the residual burst pressures of *Type IV* COPVs, based on artificially inserted damage. In field situations, the impact loads are not known, but the damage measurements can be obtained from NDT. If the NDT measurements are not precise enough, a conservative approach is to degrade all elements inside a conservative perimeter. The following conclusions were drawn from current work.

- The burst pressure of healthy vessels is calculated by the FE model. The numerical result is slightly higher than experimental values. This overestimation is most likely caused by the approximate nature of the layup that was used.

- The vessels modeled with artificial damage display a similar hoop initiated failure mode as seen from the high-speed camera. Stress concentrations were observed at the edges of inserted damages, and the failure therefore originates from the area weakened by the artificial impact damage.

- The primary effect was obtained from external fiber failures, which was also the configuration where most of the ply material was removed. The variation of delamination sizes did not

significantly alter the residual burst pressures. Also, the small crack in the internal hoop ply remained of secondary importance.

- There is a lack of suitable NDT methods to experimentally evaluate fiber failures inside the thick laminate shell (away from the surface).

ACKNOWLEDGEMENTS

The research leading to these results has received funding from the European Union's Seventh Framework Programme (FP7/2007-2013) for the Fuel Cells and Hydrogen Joint Technology Initiative under grant agreement n° 621194, http://www.hypactor.eu/. The research was also supported in part with computational resources at NTNU provided by NOTUR, http://www.sigma2.no.

REFERENCES

[1] http://hypactor.eu/.
[2] E.-H. Kim, I. Lee and T.-K. Hwang, Low-Velocity Impact and Residual Burst-Pressure Analysis of Cylindrical Composite Pressure Vessels, *AIAA Journal*, **50**, 2012, pp. 2180–93 (doi: 10.2514/1.J051515).
[3] M-G. Han and S.-H. Chang, Failure Analysis of a Type III Hydrogen Pressure Vessel under Impact Loading Induced by Free Fall, *Composite Structures*, **127**, 2015, pp. 288–97 (doi:10.1016/j.compstruct.2015.03.027).
[4] G. Perillo, F. Grytten, S. Sørbø and V. Delhaye, Numerical/experimental Impact Events on Filament Wound Composite Pressure Vessel, *Composites Part B: Engineering*, **69**, 2015, pp. 406–17 (doi: 10.1016/j.compositesb.2014.10.030).
[5] K. Lasn, N. P. Vedvik and A. T. Echtermeyer, The Sensitivity of the Burst Performance of Impact Damaged Pressure Vessels to Material Strength Properties, *IOP Conference Series: Materials Science and Engineering*, **139**, 2016, pp. 012029, (doi: 10.1088/1757-899X/139/1/012029).
[6] S. Kobayashi, Effect of Autofrettage on Durability of CFRP Composite Cylinders Subjected to out-of-Plane Loading, *Composites Part B: Engineering*, **43**, 2012, pp. 1720–26 (doi: 10.1016/j.compositesb.2012.01.032).
[7] T. Allen, S. Ahmed, P. A. S. Reed, I. Sinclair and S. M. Spearing, Understanding the Sequence of Damage in Complex Hybrid Composite Metallic Structures Subject to out-of-Plane Loading Investigated Using Computed Tomography, *Presented at the 20th International Conference on Composite Materials, 2015*.
[8] P. Blanc-Vannet, Burst Pressure Reduction of Various Thermoset Composite Pressure Vessels after Impact on the Cylindrical Part, *Composite Structures*, **160**, 2017, pp. 706–11 (doi: 10.1016/j.compstruct.2016.10.099).